

## Gap exponent of the XXZ model in a transverse field

A. Langari<sup>1,2</sup> and S. Mahdavi<sup>3</sup>

<sup>1</sup>Physics Department, Sharif University of Technology, Tehran 11365-9161, Iran

<sup>2</sup>Institute for Studies in Theoretical Physics and Mathematics (IPM), Tehran 19395-5531, Iran

<sup>3</sup>Institute for Advanced Studies in Basic Sciences, Zanjan 45195-1159, Iran

(Received 10 April 2005; revised manuscript received 7 November 2005; published 6 February 2006)

We have calculated numerically the gap exponent of the anisotropic Heisenberg model in the presence of a transverse magnetic field. We have implemented the modified Lanczos method to obtain the excited states of our model with the same accuracy as the ground state. The coefficient of the leading term in the perturbation expansion diverges in the thermodynamic limit ( $N \rightarrow \infty$ ). We have obtained the relation between this divergence and the scaling behavior of the energy gap. We have found that the opening of the gap in the presence of a transverse field scales with a critical exponent which depends on the anisotropy parameter ( $\Delta$ ). Our numerical results are in good agreement with the field theoretical approach in the whole range of the anisotropy parameter  $-1 < \Delta < 1$ .

DOI: 10.1103/PhysRevB.73.054410

PACS number(s): 75.10.Jm, 75.10.Pq, 75.40.Cx

### I. INTRODUCTION

The effect of a transverse magnetic field on low-dimensional spin systems has been attracted much interest recently from experimental and theoretical points of view. The experimental observations<sup>1,2</sup> on the quasi-one-dimensional spin-1/2 antiferromagnet  $\text{Cs}_2\text{CoCl}_4$  are a realization of the effect of a noncommuting field on the low-energy behavior of a quantum model. This shows a quantum phase transition from the spin-flop phase (ordered antiferromagnetically in the  $y$  direction) at the low magnetic field to a paramagnet for high fields. Moreover unusual-behavior has been observed in the specific heat close to the quantum critical point.<sup>2</sup> A connection between the ground state properties of the anisotropic Heisenberg model (XXZ) in the transverse field to the reported quantum phase transition has been given by the quantum renormalization group approach.<sup>3</sup> In addition, a recent mean-field approach for the weakly coupled chains<sup>4</sup> has given a very good agreement on the finite-temperature phase diagram of the two-dimensional model with the observed experimental data.<sup>1</sup>

The spin- $(s=1/2)$  Hamiltonian of the XXZ model in a transverse field on a periodic chain of  $N$  sites is

$$H = J \sum_{i=1}^N (s_i^x s_{i+1}^x + s_i^y s_{i+1}^y + \Delta s_i^z s_{i+1}^z - h s_i^x), \quad (1)$$

where  $J > 0$  is the exchange coupling in the  $XY$  easy plane,  $-1 \leq \Delta < 1$  is the anisotropy in the  $Z$  direction, and  $h$  is proportional to the transverse field. The spin ( $s_n^\alpha$ ) on site  $n$  is represented by  $\frac{1}{2} \sigma_n^\alpha$ ,  $\alpha = x, y, z$ , in terms of Pauli matrices. This model is a good candidate for explaining the low-temperature behavior of  $\text{Cs}_2\text{CoCl}_4$ . However, since the integrability of the XXZ model will be lost in the presence of a transverse field, more intensive studies from the theoretical point of view are needed.

When  $h=0$ , the XXZ model is known to be solvable and critical (gapless).<sup>5</sup> The Ising regime is governed by  $\Delta > 1$  while for  $\Delta \leq -1$  it is in the ferromagnetic phase. The mag-

netic field in the anisotropy direction commutes with the Hamiltonian at  $h=0$  and extends the gapless region (quasi-long-range order) to a border where a transition to the paramagnetic phase takes place. The model is still integrable and can be explained by a conformal field theory with central charge  $c=1$  (Ref. 6 and references therein).

Adding a transverse field to the XXZ model breaks the  $U(1)$  symmetry of the Hamiltonian to a lower, Ising-like, symmetry which develops a gap. The ground state then has long-range anti-ferromagnetic order ( $-1 < \Delta < 1$ ). However, due to nonzero projection of the order parameter on the field axis it is a spin-flop Néel state. In fact at a special field [ $h_{cl} = \sqrt{2(1+\Delta)}$ ] the ground state is known exactly to be of the classical Néel type.<sup>7,8</sup> The gap vanishes at the critical field  $h_c$ , where the transition to the paramagnetic phase occurs. The classical approach to this model reveals the mean-field result,<sup>9</sup> which is exact at  $s \rightarrow \infty$ . The implementation of the quantum renormalization group<sup>3</sup> shows that the transition at  $h_c$  is in the universality class of the Ising model in a transverse field (ITF). The phase diagram of the XYZ model in transverse field has also been presented in Ref. 3. The scaling of the gap, phase diagram, and some of the low excited states at  $h_{cl}$  of the XXZ model in the transverse field have been studied in Ref. 10. In this approach the scaling of the gap is given by the scaling of the operator  $s^x$  which is read from the asymptotic form of the correlation function<sup>11</sup> ( $\langle s_i^x s_{i+r}^x \rangle$ ). This correlation function contains two terms, an oscillating and a nonoscillating one. Each part defines a specific scaling exponent for  $s^x$  which depends on the anisotropy parameter ( $\Delta$ ).

Exact diagonalization<sup>12</sup> and density matrix renormalization group<sup>13</sup> (DMRG) results give us some knowledge on this model but not on the scaling of gap. A bosonization approach to this model in certain limits leads to a nontrivial fixed point and a gapless line which separates two gapped phases,<sup>14</sup> moreover, the connection to the axial next-nearest neighbor Ising model has been addressed. The applicability of the mean-field approximation has been studied by comparing with the DMRG results of magnetization and struc-

ture factor.<sup>15</sup> Recently the effect of a longitudinal magnetic field on both the Ising model in transverse field<sup>16</sup> and the XXZ model in the TF has been discussed.<sup>17</sup>

Here, we are going to present our numerical results on the low-energy states of the XXZ model in the transverse field which has been obtained by the modified Lanczos method introduced in Sec. II. It is believed that in this approach the accuracy of the excited state energies is the same as the ground state energy. In Sec. III, we will apply a scaling argument presented in Ref. 18 to our model and examine it by the numerical results to obtain the gap exponent. We have then applied a perturbative approach in Sec. IV to study the divergent behavior of the coefficient in the leading term of the perturbation expansion. The gap exponent has been obtained by the relation to the exponent of the diverging term. The gap exponent depends on the anisotropy parameter in agreement with the field theoretical results.<sup>10</sup> Finally, we will present the summary and discussion on our results.

## II. MODIFIED LANCZOS METHOD

The theoretical investigation of numerous physical problems requires an appropriate handling of matrices of very large rank. Even if in many applications the matrix is sparse, the problem cannot be solved by means of a direct diagonalization by standard routines. The Lanczos method and the related recursion methods,<sup>19–22</sup> possibly with appropriate implementations, have emerged as one of the most important computational procedures, mainly when a few extreme eigenvalues (largest or smallest) are desired. Grosso and Martinelli have presented a relevant implementation of the Lanczos tridiagonalization scheme,<sup>23</sup> which allows one to obtain a very fast convergence to any excited eigenvalue and eigenfunction of  $H$ , overcoming memory storage difficulties. To explain this method briefly, let us consider an operator  $H$ , with unknown eigenvalues  $E_i$  and eigenfunctions  $|\psi_i\rangle$ . Any auxiliary operator  $A=f(H)$  commutes with  $H$ , and thus shares with it a complete set of eigenfunctions corresponding to the eigenvalues  $A_i=f(E_i)$ . In order to obtain the nearest excited state of  $H$  to any *a priori* chosen trial energy  $E_r$ , we consider the auxiliary operator  $A$  in the form  $A=(H-E_r)^2$ . In a completely different context, this form is suggested by numerical analysis<sup>24</sup> to solve the Schrödinger equation within any desired energy. Now, we are faced with the solution of the following eigenvalue equation:

$$A|\psi_i\rangle \equiv (H-E_r)^2|\psi_i\rangle = \lambda_i|\psi_i\rangle. \quad (2)$$

Our strategy to solve Eq. (2) is based on the Lanczos algorithm. We briefly summarize some basic features of the Lanczos procedure in its standard formulation.

Let us denote with  $\varphi_i(i=1,2,\dots,N)$  a complete set of basis functions, for the representation of the operator  $H$  (and hence of  $A$ ). Starting from a seed state  $|u_0\rangle$ , given by whatever chosen linear combination of the  $\varphi_i$ , a set of orthonormal states  $|u_0\rangle|u_1\rangle, \dots, |u_N\rangle$  is constructed via successive applications of the operator  $A$  as follows:

$$|U_1\rangle = (A - a_0)|u_0\rangle,$$

$$a_0 = \langle u_0|A|u_0\rangle. \quad (3)$$

In general

$$|U_{n+1}\rangle = A|u_n\rangle - a_n|u_n\rangle - b_n|u_{n-1}\rangle, \quad n > 1. \quad (4)$$

The (non-normalized) state  $|U_{n+1}\rangle$  allows us to determine the coefficients  $b_{n+1}$  and  $a_{n+1}$  of the  $(n+1)$ th iteration step, via the procedure

$$b_{n+1}^2 = \langle U_{n+1}|U_{n+1}\rangle, \\ a_{n+1} = \frac{\langle U_{n+1}|A|U_{n+1}\rangle}{\langle U_{n+1}|U_{n+1}\rangle}, \quad (5)$$

where  $b_0=0$  is the initial condition. After normalization of the state  $|u_{n+1}\rangle = (1/b_{n+1})|U_{n+1}\rangle$ , the steps (4) and (5) are repeated with  $n$  replaced by  $n+1$ . In the new basis  $|u_n\rangle$ , the operator  $A$  is represented by a tridiagonal matrix  $T_m$ , whose elements  $a_n$  and  $b_n$  are explicitly known for  $m \leq N$ . The diagonalization of the tridiagonal matrix  $T_m$  gives the eigenvalues  $\lambda_i = (E_i - E_r)^2$ .

The transformation to the tridiagonal matrix is truncated at some stages because of the round-off error. However, the ground state energy can be obtained up to some significant digits. The accuracy of the excited energies is lost in the usual Lanczos method ( $A=H$ ) by the round-off error. The modified Lanczos method explained above allows us to get the higher energy levels with the same accuracy as the ground state energy. We can select the tuning parameter  $E_r$  in the range of accuracy of our method to get the excited energy levels. By choosing the appropriate  $E_r$ , we got the energy gap of the model presented in Eq. (1) up to eight digits.

## III. THE SCALING ARGUMENT AND GAP EXPONENT

The XXZ model is integrable and its low-energy properties are described by a free massless boson field theory. In the transverse magnetic field, Dimitriev *et al.* considered<sup>10</sup> the perturbed action for the model as

$$S = S_0 + h \int dt dx S^x(x,t), \quad (6)$$

where  $S_0$  is the Gaussian action of the XXZ model. The time-dependent correlation function of the XXZ chain for  $|\Delta| < 1$  has the following asymptotic form:<sup>11</sup>

$$\langle S^x(x,\tau)S^x(0,0) \rangle \sim \frac{(-1)^x A_1}{(x^2 + v^2 \tau^2)^{\theta/2}} - \frac{A_2}{(x^2 + v^2 \tau^2)^{\theta/2 + 1/2\theta}}, \quad (7)$$

where  $A_1$  and  $A_2$  are known constants,<sup>25</sup>  $\tau=it$  is the imaginary time,  $v$  is the velocity, and

$$\theta = 1 - \frac{\arccos \Delta}{\pi}. \quad (8)$$

The exponent of the energy gap ( $G$ ) has been estimated<sup>10</sup> by using the long-distance contribution of the oscillating part to the action via the scaling of  $S^x$

$$G \sim h^\mu, \quad \mu = \frac{1}{1 - \theta/2}. \quad (9)$$

If the scaling of  $S^x$  is read from the nonoscillating part of  $\langle S^x(x, \tau) S^x(0, 0) \rangle$  the contribution to the action gives the following scaling for the energy gap:<sup>26,27</sup>

$$G \sim h^\nu, \quad \nu = \frac{2}{4 - \theta - 1/\theta}. \quad (10)$$

The smaller value of  $\mu$  and  $\nu$  defines the leading order of the dependence of gap on the transverse field, the *gap exponent*. Thus,  $\mu$  is the gap exponent for  $-1 < \Delta \leq 0$  and  $\nu$  for  $0 \leq \Delta < 1$ .

We have implemented the modified Lanczos algorithm on finite-size chains ( $N=8, 10, 12, \dots, 24$ ) by using periodic boundary conditions to calculate the energy gap. We have computed the energy gap for different values of  $-1 < \Delta < 1$  and the chain lengths. The energy gap as a function of the chain length ( $N$ ) and the transverse field ( $h$ ) is defined as

$$G(N, h) = E_2(N, h) - E_0(N, h), \quad (11)$$

where  $E_0$  is the ground state energy and  $E_2$  is the second excited state one. The first excited state crosses the ground state  $N/2$  times for a finite chain and the last crossing occurs at the classical point<sup>10</sup>  $h_{cl} = \sqrt{2(1+\Delta)}$ . These two states form a twofold-degenerate ground state in the thermodynamic limit where  $E_1 - E_0$  vanishes.

In the case of  $h$  equals zero, the spectrum of the XXZ model is gapless. The gap vanishes in the thermodynamic limit proportional to the inverse of the chain length,

$$\lim_{N \rightarrow \infty} G(N, h=0) \rightarrow \frac{B}{N}. \quad (12)$$

The coefficient  $B$  is known exactly from the Bethe ansatz solution.<sup>28</sup> We consider this equation as the initial condition for our procedure.<sup>18</sup> Adding the transverse field to the Hamiltonian, a nonzero gap develops. The presence of the gap can be characterized by the following expression:

$$\frac{G(N, h)}{G(N, 0)} = 1 + f(x), \quad (13)$$

in the combined limit

$$N \rightarrow \infty, \quad h \rightarrow 0, \quad (14)$$

where  $x = Nh^\varepsilon$  is fixed and  $f(x)$  is the scaling function. Thus, the gap at finite  $h$  can be defined

$$G(N, h) = \frac{B}{N} + \frac{B}{N} f(x) \equiv \frac{B}{N} + g(N)h^\varepsilon, \quad (15)$$

where  $g(N)$  is a function of only  $N$ . It is imposed that the function  $g(N)$  approaches a nonzero constant value in the thermodynamic limit:  $\lim_{N \rightarrow \infty} g(N) = \text{const} \equiv C_\infty$ . The regime where we can observe the scaling of the gap is in the thermodynamic limit ( $N \rightarrow \infty$ ) and a very small value of  $h$  ( $h \ll 1$ ). This means that the scaling behavior is observable at large  $x$  ( $x = Nh^\varepsilon \gg 1$ ). The asymptotic behavior of  $g(N)$  for

$N \rightarrow \infty$  defines that the large- $x$  behavior of  $f(x)$  must be proportional to  $x$ ,

$$f(x) = \frac{g(N)}{B} x \Rightarrow \lim_{x \gg 1} f(x) = \frac{C_\infty}{B} x. \quad (16)$$

Thus, if we consider the asymptotic behavior of  $f(x)$  as

$$f(x) \sim x^\phi, \quad (17)$$

the  $\phi$  exponent must be equal to 1 ( $\phi=1$ ). If we multiply both sides of Eq. (15) by  $N$  we get

$$\lim_{N \rightarrow \infty (x \gg 1)} NG(N, h) = B + C_\infty x. \quad (18)$$

Equation (18) shows that the large- $x$  behavior of  $NG(N, h)$  is linear in  $x$  where the scaling exponent of the energy gap is  $\varepsilon$ .

We have plotted the values of  $NG(N, h)$  versus  $Nh^\varepsilon$  for  $\Delta=0.5, -0.5$  in Fig. 1. The reported results have been computed on a chain of length  $N=18, 20, 22, 24$  with periodic boundary conditions. According to Eq. (18), it can be seen from our numerical results presented in Figs. 1(a) and 1(b) that the linear behavior is very well satisfied by  $\varepsilon=2.0$ . But the data do not show a scale invariance plot for different  $N$ , which is expected from the scaling behavior. We have also implemented our numerical tool to calculate the exponent of the energy gap at  $\Delta=0, 0.25, -0.25$ . Again, the plot of  $NG(N, h)$  versus  $Nh^\varepsilon$  shows a linear behavior for  $\varepsilon=2.0$ .

However, we should note that the horizontal axes presented in Fig. 1 are limited to very small values of  $x = Nh^\varepsilon < 0.0024$ . Thus, we are not allowed to read the scaling exponent of the gap which exists in the thermodynamic limit ( $N \rightarrow \infty$  or  $x \gg 1$ ). We have been limited to consider the maximum value of  $N=24$ , because for the present model [Eq. (1)] the total  $S^z$  does not commute with the Hamiltonian and we should consider the full Hilbert space of  $2^N$  in our computations. Moreover, to avoid the effect of level crossings, we should consider very small values of  $h < 0.01$ . Therefore, the value of  $x$  cannot be increased in this method. We will face the same problem even if the calculation is done by density matrix renormalization group. In that case we can extend the calculation for larger sizes,  $N \sim 100$ , but the first level crossing happens for a smaller value of  $h$ . The position of the first level crossing is proportional to  $N^{-1/\varepsilon}$  which will be explained in the next sections. This is the level crossing between the higher excited states, in this case between the second and third ones. Thus, we have to find the scaling behavior from the small- $x$  data.

#### IV. PERTURBATIVE APPROACH

According to our computations where  $N \leq 24$ , the small- $x$  regime is equivalent to very small  $h$  values. In this case, the energy gap of the finite-size system is basically representing the perturbative behavior. Thus, Eq. (15) is rewritten in the form

$$G(N, h) = \frac{B}{N} + \frac{B}{N} f(x) \equiv \frac{B}{N} + g(N)h^2, \quad (19)$$

to a very good approximation, because the first-order perturbation correction is zero in the transverse field and the lead-

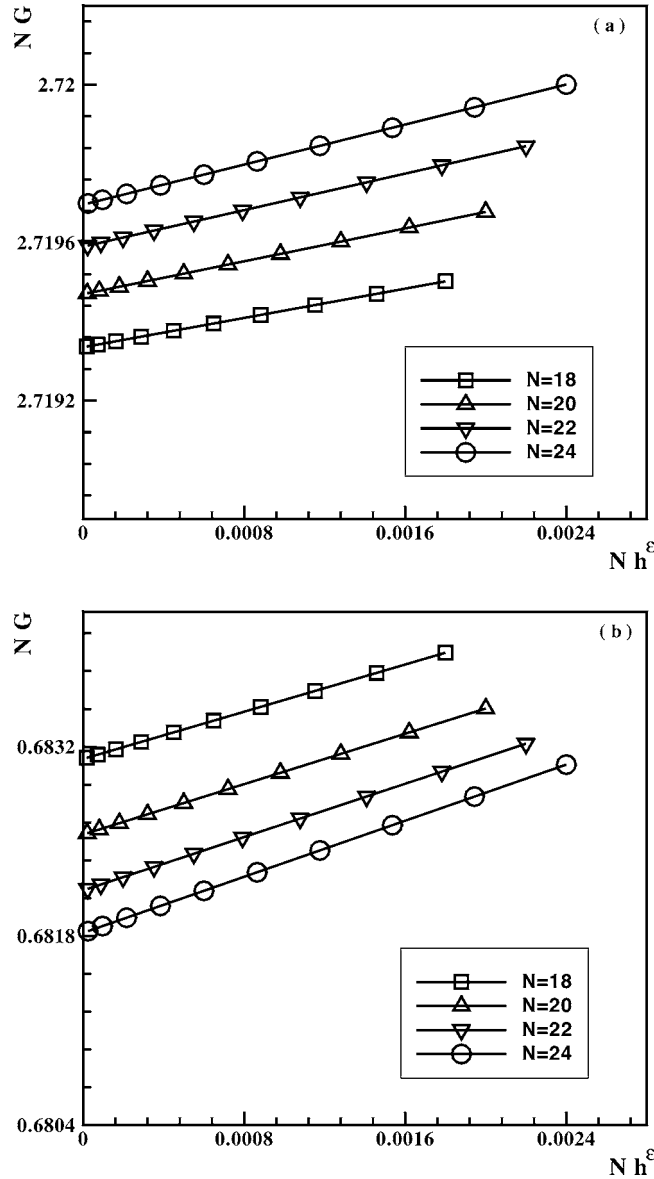


FIG. 1. The product of energy gap and chain length ( $NG$ ) versus  $Nh^\varepsilon$ .  $\Delta=(a)$  0.5 and (b)  $-0.5$ . A linear behavior is obtained by choosing  $\varepsilon=2.0$  for all different chain lengths  $N=18, 20, 22, 24$ . The solid lines are guides for the eye.

ing nonzero term is  $h^2$ . In this way we get  $g(N) = Bf(x)/Nh^2$ . If the small- $x$  behavior of the scaling function is defined by  $f(x) \sim x^{\phi_s}$  we find that

$$g(N) = BN^{(\phi_s-1)}h^{(\varepsilon\phi_s-2)}. \quad (20)$$

Since  $g(N)$  is a function of only  $N$  we end up with

$$\varepsilon\phi_s = 2. \quad (21)$$

Multiplication of both sides of Eq. (19) by  $N$  leads to  $NG(N, h) = B + Bx^{2/\varepsilon}$ . This shows that in the small- $x$  regime,  $NG(N, h)$  is a linear function of  $x^{2/\varepsilon}$ . This is in agreement with our data in Fig. 1 where  $\phi_s=1$  and according to Eq. (21), the value of  $\varepsilon$  is found to be  $\varepsilon=2$ .

The function  $g(N)$  in Eq. (19) is actually the coefficient of the first nonzero correction in the perturbation expansion for the energy gap of a finite chain,

$$G(N, h) = G(N, 0) + g_1(N)h^2 + \cdots + g_m(N)h^{2m} \\ = \frac{B}{N} + g_1(N)h^2 + \cdots + g_m(N)h^{2m} \quad (22)$$

where  $m$  is an integer. The effect of higher-order terms can be neglected for  $h \leq 0.01$  to a very good approximation. Now, let us consider that the large- $N$  behavior of  $g_1(N)$  is

$$\lim_{N \rightarrow \infty} g_1(N) \approx a_1 N^\alpha. \quad (23)$$

We find that

$$G(N, h) \approx \frac{B}{N}(1 + b_1 N^{\alpha+1} h^2), \quad (24)$$

where  $b_1 = a_1/B = \text{const.}$  We can write Eq. (24) in terms of the scaling variable ( $x = Nh^\varepsilon$ ),

$$\frac{G(N, h)}{B/N} \approx 1 + N^{\alpha+1-2/\varepsilon} x^{2/\varepsilon}. \quad (25)$$

For the large- $N$  limit, Eq. (25) should be independent of  $N$ . This imposes the following relation:

$$\alpha + 1 - \frac{2}{\varepsilon} = 0. \quad (26)$$

This equation defines the relation between  $\alpha$  and  $\varepsilon$ ,

$$\varepsilon = \frac{2}{\alpha + 1}. \quad (27)$$

The above arguments propose to look for the large- $N$  behavior of  $g_1(N)$ . For this purpose, we have plotted in Fig. 2 the following expression versus  $N$ :

$$g_1(N) \approx \frac{G(N, h) - G(N, 0)}{h^2}, \quad (28)$$

for fixed values of  $h$  ( $0.001 \leq h \leq 0.01$ ) and  $\Delta = 0.5, -0.5$ . The results have been plotted for different sizes,  $N = 12, 14, \dots, 24$  to derive the  $\alpha$  exponent defined in Eq.(23). In Fig. 2(a) we have considered the case of  $\Delta = 0.5$  and found the best fit to our data for  $\alpha = 0.88 \pm 0.02$ . Therefore,  $\varepsilon = 1.06 \pm 0.02$  which shows a very good agreement with Eq. (10),  $\varepsilon_{FT} = \nu = 12/11 = 1.09$ . Moreover, our data for different  $h$  values fall perfectly on each other, which shows that our results for  $g_1(N)$  are independent of  $h$  as we have expected. We have also plotted the results for  $\Delta = -0.5$  in Fig. 2(b) and found  $\alpha = 0.55 \pm 0.02$ . Then we obtain  $\varepsilon = 1.29 \pm 0.02$  which can be compared with Eq. (9),  $\varepsilon_{FT} = \mu = 6/5 = 1.2$ . This shows a slight deviation which is the result of numerical computations and also the limitation on the size of system. Moreover, the magnitude of the energy gap is smaller for  $\Delta = -0.5$  than in the case of  $\Delta = 0.5$ , which implies less accuracy. However, the results for different  $h$ , give once more a unique  $g_1(N)$  in agreement with its definition to be independent of  $h$ .

We have extended our numerical computations to consider other values of  $\Delta$ . The results have been presented in

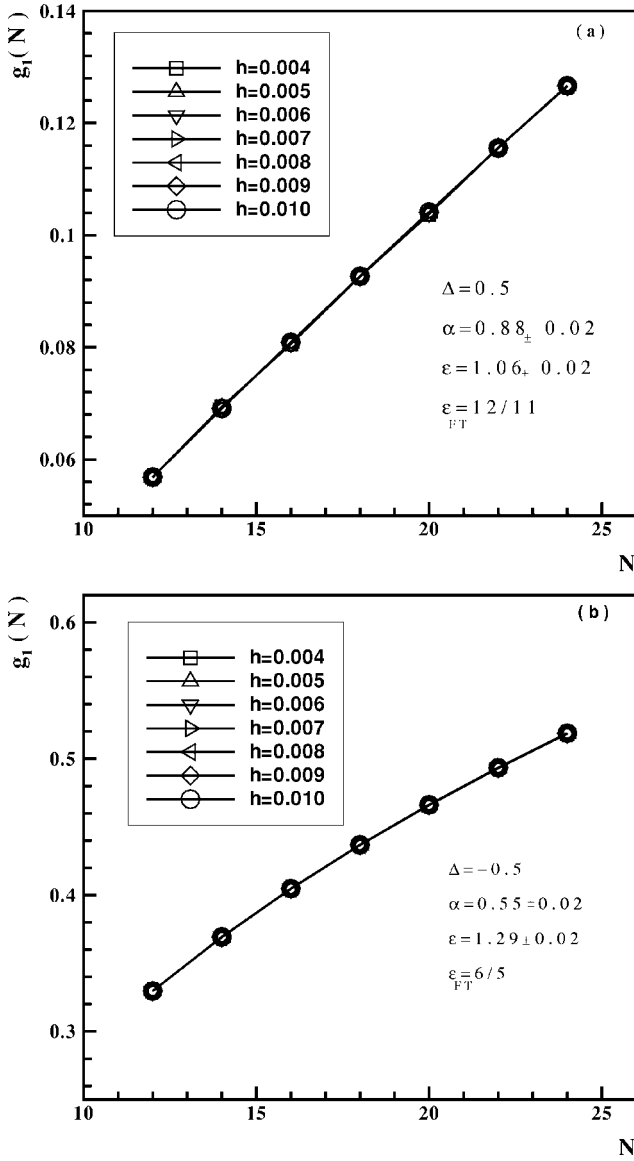


FIG. 2. The value of  $g_1(N)$  versus the chain length ( $N$ ).  $\Delta=(a)$  0.5 and (b)  $-0.5$ . Data for different transverse fields  $0.004 \leq h \leq 0.01$  fall exactly on each other.

Table I. We have listed  $\alpha$ , the resulting  $\varepsilon$  that is obtained from Eq. (27), and the result of the field theoretical approach ( $\varepsilon_{FT}$ ) for different values of  $\Delta$ . Our numerical results show very good agreement with the exponents derived in the field theoretical approach.<sup>10</sup>

## V. DISCUSSION AND SUMMARY

We have studied the opening of the excitation gap of the XXZ chain by breaking the rotational symmetry. We have implemented the modified Lanczos method to get the excited state energies at the same accuracy as the ground state one. The convergence of this method is fast for the low-energy states but gets slower for higher-energy ones. The reason is related to the condensation of states in a fixed interval of energy by going to higher states. Thus the method will be

TABLE I. The  $\alpha$  exponent defined in Eq. (23), the related gap exponent ( $\varepsilon$ ), and the corresponding value  $\varepsilon_{FT}$  obtained by the field theoretical approach for different anisotropy parameters ( $\Delta$ ).

$\Delta$	$\alpha$	$\varepsilon$	$\varepsilon_{FT}$
0.70	0.96	1.02	1.04
0.50	0.88	1.06	1.09
0.25	0.70	1.17	1.18
0.0	0.65	1.21	1.33
-0.25	0.60	1.25	1.26
-0.50	0.55	1.29	1.20
-0.70	0.59	1.25	1.14

very sensitive to the initial parameter  $E_t$  [Eq. (2)]. However, for the tenth lowest-energy state we got fast convergence. We have been limited to consider the maximum  $N=24$ , because for the present model [Eq. (1)] the total  $S^z$  does not commute with the Hamiltonian. Thus, we should consider the full Hilbert space of  $2^N$  in our computations.

We have tried to find the scaling of the energy gap in the presence of the transverse field by introducing the scaling function in Eq. (13). According to this approach, the energy gap scales as  $G \sim h^\varepsilon$  where  $\varepsilon$  defines  $x=Nh^\varepsilon$ , the scaling variable. The right scaling exponent gives a linear behavior of  $NG(N, h)$  versus  $x$  for large  $x$ . To find the large- $x$  behavior we have faced a serious problem. To see the scaling behavior we have to consider very small values of  $h$  to avoid the effect of level crossing between the excited state that defines the gap and the upper states. The position of the first level crossing is roughly proportional to the inverse of the chain length. Thus, we were not able to get the large- $x$  behavior and be far from the crossing point at the same time.

The limitation to very small  $h$  values states that our results are representing the perturbative ones. We are then led to get the scaling behavior by finding the divergence of  $g_1(N) \sim N^\alpha$  in the thermodynamic limit ( $N \rightarrow \infty$ ). The function  $g_1(N)$  is the coefficient of the leading term in the perturbation expansion [Eq. (22)]. Based on the formulation presented in the previous section the gap exponent is related to the divergence of  $g_1(N)$  by  $\varepsilon=2/(\alpha+1)$ . Our numerical results presented in Fig. 2 show that  $g_1(N)$  is independent of  $h$  and its divergence versus  $N$  is defined by Eq. (23). Moreover, the gap exponent that has been obtained by our numerics (listed in Table I) is in very good agreement with the results obtained by the field theoretical approach.<sup>10</sup>

We might also find the gap exponent by finding the precise location of the first level crossing between the second and third excited states, which we call  $h_1$ . The slope of  $\log(h_1)$  versus  $\log(N)$  is  $-1/\varepsilon$ . In the small- $h$  regime where Eq. (22) is approximated up to the quadratic term, we can write two different expressions for the energy of the third and second excited states, namely,

$$E_3(N, h) - E_0(N, h) = G_3(N, h=0) + g_1^{(3)}(N)h^2,$$

$$E_2(N, h) - E_0(N, h) = G_2(N, h=0) + g_1^{(2)}(N)h^2. \quad (29)$$

The subtraction of the two terms give the difference of  $E_3 - E_2$  which is a function of the terms presented in the right sides of Eq. (29). The zero-field terms are proportional to  $N^{-1}$  and the coefficients of the quadratic terms obey Eq. (23). Thus, the scaling of  $h_1$  in terms of the lattice size is like  $h_1 \sim N^{-1/\varepsilon}$ . However, the preceise determination of  $h_1$  defines the accuracy of this approach.

## ACKNOWLEDGMENTS

The authors would like to thank K.-H. Mütter, A. Fledderjohann, M. Karbach, I. Peschel, and G. Japaridze for their valuable comments and discussions. A.L. would like to acknowledge the Institute for Advanced Studies in Basic Sciences where the initial part of this work was started.

- 
- <sup>1</sup>M. Kenzelmann, R. Coldea, D. A. Tennant, D. Visser, M. Hofmann, P. Smeibidl, and Z. Tylczynski, Phys. Rev. B **65**, 144432 (2002).
- <sup>2</sup>T. Radu (private communication).
- <sup>3</sup>A. Langari, Phys. Rev. B **69**, 100402(R) (2004).
- <sup>4</sup>D. V. Dmitriev and V. Ya. Krivnov, cond-mat/0407203 (unpublished).
- <sup>5</sup>C. N. Yang and C. P. Yang Phys. Rev. **150**, 321 (1966); **150**, 327 (1966).
- <sup>6</sup>F. C. Alcaraz and A. L. Malvezzi, J. Phys. A **28**, 1521 (1995); M. Tsukano and K. Nomura, J. Photogr. Sci. **67**, 302 (1998).
- <sup>7</sup>G. Müller and R. E. Shrock, Phys. Rev. B **32**, 5845 (1985).
- <sup>8</sup>S. Mori, I. Mannari, and I. Harda, J. Phys. Soc. Jpn. **63**, 3474 (1994).
- <sup>9</sup>J. Kurmann, H. Thomas, and G. Müller, Physica A **112**, 235 (1982).
- <sup>10</sup>D. V. Dmitriev, V. Ya. Krivnov, and A. A. Ovchinnikov, Phys. Rev. B **65**, 172409 (2002); D. V. Dmitriev, V. Ya. Krivnov, A. A. Ovchinnikov, and A. Langari, JETP **95**, 538 (2002).
- <sup>11</sup>A. Luther and I. Peschel, Phys. Rev. B **12**, 3908 (1975).
- <sup>12</sup>S. Mori, J. -J. Kim, and I. Harda, J. Phys. Soc. Jpn. **64**, 3409 (1995).
- <sup>13</sup>F. Capraro and C. Gros, Eur. Phys. J. B **29**, 35 (2002).
- <sup>14</sup>A. Dutta and D. Sen, Phys. Rev. B **67**, 094435 (2003).
- <sup>15</sup>J. -S. Caux, F. H.L. Essler, and U. Löw, Phys. Rev. B **68**, 134431 (2003).
- <sup>16</sup>A. A. Ovchinnikov, D. V. Dmitriev, V. Ya. Krivnov, and V. O. Cheranovskii, Phys. Rev. B **68**, 214406 (2003).
- <sup>17</sup>D. V. Dmitriev and V. Ya. Krivnov, cond-mat/0403035 (unpublished).
- <sup>18</sup>A. Fledderjohann, M. Karbach, and K. -H. Mütter, Eur. Phys. J. B **5**, 487 (1998).
- <sup>19</sup>C. Lanczos, J. Res. Natl. Bur. Stand. **45**, 255 (1950).
- <sup>20</sup>R. Haydock, V. Heine, and M. J. Kelly, J. Phys. C **5**, 2845 (1972); **8**, 2591 (1975).
- <sup>21</sup>G. Grosso and G. Pastori Parravicini, Adv. Chem. Phys. **62**, 81133 (1985).
- <sup>22</sup>H. Q. Lin and J. E. Gubernatis, Comput. Phys. **7**, 400 (1993).
- <sup>23</sup>G. Grosso, L. Martinelli, and G. Pastori Parravicini, Phys. Rev. B **51**, 13033 (1995).
- <sup>24</sup>J. C. Nash, *Compact Numerical Methods for Computers* (Hilger, Bristol, 1979).
- <sup>25</sup>T. Hikihara and A. Furusaiki, Phys. Rev. B **58**, R583 (1998).
- <sup>26</sup>A. O. Gogolin, A. A. Nersesyan, and A. M. Tsvelik, *Bosonization and Strongly Correlated Systems* (Cambridge University Press, Cambridge, U.K., 1998).
- <sup>27</sup>A. A. Nersesyan, A. Luther, and F. V. Kusmartsev, Phys. Lett. A **176**, 363 (1993).
- <sup>28</sup>A. Klümper, Eur. Phys. J. B **5**, 677 (1998), and references therein.